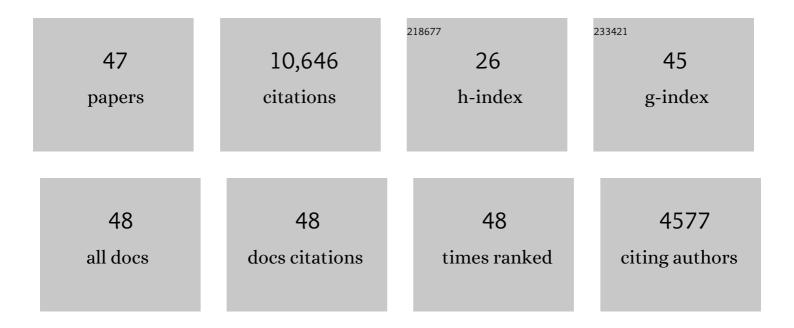
Jeff D Vervoort

List of Publications by Year in descending order

Source: https://exaly.com/author-pdf/2940048/publications.pdf Version: 2024-02-01



#	Article	IF	CITATIONS
1	The Lu–Hf and Sm–Nd isotopic composition of CHUR: Constraints from unequilibrated chondrites and implications for the bulk composition of terrestrial planets. Earth and Planetary Science Letters, 2008, 273, 48-57.	4.4	2,427
2	The 176Lu decay constant determined by Lu–Hf and U–Pb isotope systematics of Precambrian mafic intrusions. Earth and Planetary Science Letters, 2004, 219, 311-324.	4.4	2,304
3	Evolution of the depleted mantle: Hf isotope evidence from juvenile rocks through time. Geochimica Et Cosmochimica Acta, 1999, 63, 533-556.	3.9	1,263
4	Relationships between Lu–Hf and Sm–Nd isotopic systems in the global sedimentary system. Earth and Planetary Science Letters, 1999, 168, 79-99.	4.4	936
5	The Hf–Nd isotopic composition of marine sediments. Geochimica Et Cosmochimica Acta, 2011, 75, 5903-5926.	3.9	449
6	lsotopic composition of Yb and the determination of Lu concentrations and Lu/Hf ratios by isotope dilution using MC-ICPMS. Geochemistry, Geophysics, Geosystems, 2004, 5, n/a-n/a.	2.5	430
7	Hadean crustal evolution revisited: New constraints from Pb–Hf isotope systematics of the Jack Hills zircons. Earth and Planetary Science Letters, 2010, 296, 45-56.	4.4	412
8	Constraints on early Earth differentiation from hafnium and neodymium isotopes. Nature, 1996, 379, 624-627.	27.8	316
9	Origin of Mesoproterozoic A-type granites in Laurentia: Hf isotope evidence. Earth and Planetary Science Letters, 2006, 243, 711-731.	4.4	264
10	Clarifying the zircon Hf isotope record of crust–mantle evolution. Chemical Geology, 2016, 425, 65-75.	3.3	242
11	U–Pb baddeleyite ages and Hf, Nd isotope chemistry constraining repeated mafic magmatism in the Fennoscandian Shield from 1.6 to 0.9ÂGa. Contributions To Mineralogy and Petrology, 2005, 150, 174-194.	3.1	192
12	Migrating magmatism in the northern US Cordillera: in situ U–Pb geochronology of the Idaho batholith. Contributions To Mineralogy and Petrology, 2010, 159, 863-883.	3.1	134
13	Isotopic Evolution of the Idaho Batholith and Challis Intrusive Province, Northern US Cordillera. Journal of Petrology, 2011, 52, 2397-2429.	2.8	133
14	Coupled Lu–Hf and Sm–Nd geochronology constrains garnet growth in ultraâ€highâ€pressure eclogites from the Dabie orogen. Journal of Metamorphic Geology, 2008, 26, 741-758.	3.4	124
15	Subduction factory processes beneath the Guguan cross-chain, Mariana Arc: no role for sediments, are serpentinites important?. Contributions To Mineralogy and Petrology, 2006, 151, 202-221.	3.1	117
16	Using the magmatic record to constrain the growth of continental crust—The Eoarchean zircon Hf record of Greenland. Earth and Planetary Science Letters, 2018, 488, 79-91.	4.4	110
17	Halogens, trace element concentrations, and Sr-Nd isotopes in apatite from iron oxide-apatite (IOA) deposits in the Chilean iron belt: Evidence for magmatic and hydrothermal stages of mineralization. Geochimica Et Cosmochimica Acta, 2019, 246, 515-540.	3.9	84
18	Coupled zircon Lu–Hf and U–Pb isotopic analyses of the oldest terrestrial crust, the >4.03 Ga Acasta Gneiss Complex. Earth and Planetary Science Letters, 2017, 458, 37-48.	4.4	83

JEFF D VERVOORT

#	Article	IF	CITATIONS
19	Probing for Proterozoic and Archean crust in the northern U.S. Cordillera with inherited zircon from the Idaho batholith. Bulletin of the Geological Society of America, 2013, 125, 73-88.	3.3	62
20	Insights into the metamorphic evolution of the Belt–Purcell basin; evidence from Lu–Hf garnet geochronology. Canadian Journal of Earth Sciences, 2010, 47, 161-179.	1.3	58
21	Hafnium and neodymium isotope variations in NE Atlantic seawater. Geochemistry, Geophysics, Geosystems, 2009, 10, .	2.5	49
22	Laser ablation split-stream analysis of the Sm-Nd and U-Pb isotope compositions of monazite, titanite, and apatite – Improvements, potential reference materials, and application to the Archean Saglek Block gneisses. Chemical Geology, 2020, 539, 119493.	3.3	42
23	Combining Nd isotopes in monazite and Hf isotopes in zircon to understand complex open-system processes in granitic magmas. Geology, 2017, 45, 267-270.	4.4	40
24	Constraints on the timing and duration of orogenic events by combined Lu–Hf and Sm–Nd geochronology: An example from the Grenville orogeny. Earth and Planetary Science Letters, 2018, 501, 152-164.	4.4	34
25	Deciphering the zircon Hf isotope systematics of Eoarchean gneisses from Greenland: Implications for ancient crust-mantle differentiation and Pb isotope controversies. Geochimica Et Cosmochimica Acta, 2019, 250, 76-97.	3.9	33
26	Disturbances in the Sm–Nd isotope system of the Acasta Gneiss Complex—Implications for the Nd isotope record of the early Earth. Earth and Planetary Science Letters, 2020, 530, 115900.	4.4	33
27	Origins of the terrestrial Hf-Nd mantle array: Evidence from a combined geodynamical-geochemical approach. Earth and Planetary Science Letters, 2019, 518, 26-39.	4.4	26
28	Petrochronology of Wadi Tayin Metamorphic Sole Metasediment, With Implications for the Thermal and Tectonic Evolution of the Samail Ophiolite (Oman/UAE). Tectonics, 2020, 39, e2020TC006135.	2.8	24
29	Timescales of collisional metamorphism from Sm-Nd, Lu-Hf and U-Pb thermochronology: A case from the Proterozoic Putumayo Orogen of Amazonia. Geochimica Et Cosmochimica Acta, 2018, 235, 103-126.	3.9	21
30	Evolution of the Jura-Cretaceous North American Cordilleran margin: Insights from detrital-zircon U-Pb and Hf isotopes of sedimentary units of the North Cascades Range, Washington. , 2017, 13, 2094-2118.		20
31	Pressure-temperature-time paths from the Funeral Mountains, California, reveal Jurassic retroarc underthrusting during early Sevier orogenesis. Bulletin of the Geological Society of America, 2020, 132, 1047-1065.	3.3	19
32	The coupled Hf-Nd isotope record of the early Earth in the Pilbara Craton. Earth and Planetary Science Letters, 2021, 572, 117139.	4.4	19
33	Reconciliation of discrepant U–Pb, Lu–Hf, Sm–Nd, Ar–Ar and U–Th/He dates in an amphibolite from the Cathaysia Block in Southern China. Contributions To Mineralogy and Petrology, 2020, 175, 1.	3.1	17
34	Transfer of Metasupracrustal Rocks to Midcrustal Depths in the North Cascades Continental Magmatic Arc, Skagit Gneiss Complex, Washington. Tectonics, 2017, 36, 3254-3276.	2.8	15
35	Nd isotope re-equilibration during high temperature metamorphism across an orogenic belt: Evidence from monazite and garnet. Chemical Geology, 2020, 551, 119751.	3.3	15
36	Tectonic evolution of the Grenville Orogen in the central Appalachians. Precambrian Research, 2020, 346, 105740.	2.7	15

JEFF D VERVOORT

#	Article	IF	CITATIONS
37	Combined Sm-Nd, Lu-Hf, and 142Nd study of Paleoarchean basalts from the East Pilbara Terrane, Western Australia. Chemical Geology, 2021, 578, 120301.	3.3	14
38	Tracking long-distance atmospheric deposition of trace metal emissions from smelters in the upper Columbia River valley using Pb isotope analysis of lake sediments. Environmental Science and Pollution Research, 2018, 25, 5501-5513.	5.3	12
39	Magmatic-tectonic control on the generation of silicic magmas in Iceland: Constraints from Hafnarfjall-Skarðsheiði volcano. Lithos, 2018, 318-319, 326-339.	1.4	11
40	Bioavailability and uptake of smelter emissions in freshwater zooplankton in northeastern Washington, USA lakes using Pb isotope analysis and trace metal concentrations. Environmental Pollution, 2018, 238, 348-358.	7.5	10
41	Unraveling the complexity of zircons from the 4.0–2.9â€ ⁻ Ca Acasta Gneiss Complex. Geochimica Et Cosmochimica Acta, 2020, 283, 85-102.	3.9	10
42	Dating Continental Subduction Beneath the Samail Ophiolite: Garnet, Zircon, and Rutile Petrochronology of the As Sifah Eclogites, NE Oman. Journal of Geophysical Research: Solid Earth, 2021, 126, e2021JB022715.	3.4	9
43	Integrated garnet and zircon–titanite geochronology constrains the evolution of ultraâ€high–pressure terranes: An example from the Sulu orogen. Journal of Metamorphic Geology, 2019, 37, 611-631.	3.4	4
44	Long-lived anatexis in the exhumed middle crust of the Torngat Orogen: Constraints from phase equilibria modeling and garnet, zircon, and monazite geochronology. Lithos, 2021, 388-389, 106022.	1.4	4
45	Reconciling Garnet Lu–Hf and Sm–Nd and Monazite U–Pb Ages for a Prolonged Metamorphic Event, Northern New Mexico. Journal of Petrology, 2022, 63, .	2.8	4
46	Integrated garnet and zircon petrochronology reveals the timing and duration of orogenic events in the North China Craton. Lithos, 2021, 382-383, 105939.	1.4	3
47	Petrogenesis of voluminous silicic magmas in the Sierra Madre Occidental large igneous province, Mexican Cordillera: Insights from zircon and Hf-O isotopes. , 0, , .		2